



Oily Wastewater Remediation using Polyurethane Sponges Coated with an Optimised Amount of Graphene Nanoplatelets

Stella Mitchell¹, Jiun Hor Low^{1, 2, 3, *} and Li Wan Yoon⁴

¹School of Engineering, Faculty of Innovation and Technology, Taylor's University, No.1, Jalan Taylor's, 47500 Subang Jaya, Selangor, Malaysia

²Clean Technology Impact Lab, Taylor's University, No.1, Jalan Taylor's, 47500 Subang Jaya, Selangor, Malaysia

³Centre for Sustainable Societies, Taylor's University, No.1, Jalan Taylor's, 47500 Subang Jaya, Selangor, Malaysia

⁴Department of Engineering, School of Engineering and Technology, Sunway University, Bandar Sunway, Selangor 47500, Malaysia

*Corresponding author: JiunHor.Low@taylors.edu.my

Received 26 March 2025

Revised 4 June 2025

Accepted 17 September 2025

Abstract

Oily wastewater discharged into water bodies without proper treatment can endanger aquatic ecosystems and human health. This study explored an alternative method for treating oily wastewater using a graphene-nanoplatelet (GNP)-coated polyurethane (PU) sponge and reported its oil absorption performance. The PU sponge surface was modified by dip-coating it with 0 g, 0.5 g, 1 g, 1.5 g, 2 g, and 2.5 g GNP aqueous suspension to prepare a GNP-coated PU sponge. Fourier-transform infrared (FTIR) spectroscopy demonstrated that the GNP successfully coated onto the PU sponge surface. The GNP coating conferred a selective absorption ability to the PU sponges, which significantly enhanced their hydrophobicity and oleophilicity. The use of 1 g GNP achieved the highest oil absorption, which was approximately 44 times the original PU sponge mass. The morphological analysis confirmed that the GNP even dispersion on the PU sponge surface was the main reason for the oil absorption being highest at 1 g GNP. The results suggested that 1 g GNP should be used for modifying PU sponge surfaces for treating oily wastewater. Furthermore, the results provided fundamental knowledge and information that can facilitate the design and development of a GNP- and PU sponge-based material for treating oily wastewater.

Keywords: Advanced material, Advanced wastewater treatment, Carbon nanomaterial, Nanotechnology in wastewater treatment

1. Introduction

The fossil fuel and crude oil-based product market has increased, as scientific advancements have increased the number of products containing crude oil as their primary feed, such as waxes, synthetic flavours, scents, lubricating oils, and tars [1]. This increase has necessitated the routine offshore transportation of oil or organic fluids from the production to consumption points. Consequently, the risk of maritime oil leaks has increased. Additionally, oil leakage or illegal industrial discharges can cause oil spill water pollution. Oil spills create oil slicks on the water surface, which endanger life below the surface by blocking sunlight and reducing the oxygen concentration in the water. Furthermore, oil-polluted water has adverse effects on the marine food chain and leads to bioaccumulation. Hence, consuming these contaminated seafoods and water would endanger human health. Accordingly, effectively removing harmful petrochemicals and oils from water to maintain the environment is urgent and crucial [2].

Wastewater can be treated with various treatments, which involve physical, chemical, or biological methods. Physical separation procedures include filtration, reverse osmosis, gravity separation, adsorption, and electrodialysis. Nevertheless, such methods are time- and cost-consuming and require high amounts of energy.

Chemical treatment methods include chemical coagulation and chemical oxidation. Lastly, biological treatment treats wastewater through activated sludge treatment and biofilters. These methods are effective but subject to significant disadvantages. For example, chemical procedures frequently create a toxic environment in the area where the chemical has been used, such as pH imbalance or toxic harm to marine life [3]. While biological approaches are preferable as they are sustainable and cost-efficient for separating oil and water, they are not as effective as physical and chemical methods [4].

Contrasting with the aforementioned methods, three-dimensional (3D) porous materials have large surface areas and well-developed pores, which render them promising candidates as high-capacity absorbing materials to treat wastewater through absorption [5]. Polyurethane (PU) sponges are a highly porous 3D material that can potentially be used as a base component for separating oil from water as it has high elasticity, elastic recovery, substantial surface area, and low weight as an absorbent. Nonetheless, PU sponge cannot be directly used for oil-water separation without surface modification as it does not have a selective absorption ability to effectively solely separate oil from oily wastewater. Thus, the use of hydrophobic graphene, a two-dimensional (2D) carbon material [6], to modify hydrophilic PU sponges has been researched [5]. The investigations successfully coated graphene onto the PU sponge surface to modify it for treating oily wastewater.

The idea has been extended to the use of graphene oxide, a chemically oxidised form of graphene [7,8], whereby a superhydrophobic PU sponge was developed for oil-water separation [9,10]. Graphene nanoplatelets (GNP) are an alternative hydrophobic carbon nanomaterial that can also be explored to modify the PU sponge surface for oily wastewater treatment. The GNP is composed of stacked platelet-shaped graphene sheets. The unique size and morphology of these nanoscale stacks allow the GNP to be easily dispersed into other materials, which yields higher-value composites enhanced by the exceptional mechanical, thermal, and electrical properties of graphene [11]. Furthermore, the ease and low cost of manufacturing GNP have rendered it an emerging nanofiller compared to graphene, graphene oxide, and other graphene derivatives [12,13]. The fascinating properties and economic attractiveness of GNP are compelling reasons for developing more advanced GNP-based materials for different applications. Nonetheless, reports on PU sponge surface modification using GNP for oily wastewater treatment remain limited. Moreover, the effect of the amount of GNP used on the PU sponge properties and oil removal performance also remains unclear. Therefore, this knowledge gap should be addressed.

This study investigated the effects of GNP on the properties of modified PU sponge surfaces for oily wastewater separation. The Fourier-transform infrared (FTIR) spectroscopy, water absorption, oil absorption, and surface morphology of the GNP-coated PU sponges are reported and the suitable amount of GNP to be used was identified in the present study. These results should be able to guide the development of an alternative method to treat oily wastewater based on the use of the nanocomposite developed based on GNP and PU sponges.

2. Materials and methods

2.1 Materials

The GNP confirmation of acceptance for studies (CAS) (CAS No.: 7782-42-5; 2–10 nm thickness and 2–7 μm diameter) was supplied by acute coronary syndrome (ACS) Material limited liability company (LLC). The PU sponge was acquired from the local market in Melaka, Malaysia. Absolute ethanol (99.5%) (w/w) (SYSTERM, CAS No.: 64-17-5) was purchased from Classic Chemicals Sdn. Bhd. The oil absorption capacity testing used SAJI palm cooking oil (Delima Oil Products Sdn. Bhd.) and PETRONAS Mach 5 SAE 40 engine oil [PETRONAS Lubricants International (PLI)].

2.2 Preparation of GNP-coated PU sponges

The PU sponge was cut into 3 cm \times 2 cm \times 2.5 cm blocks, cleaned with the absolute ethanol for 30 minutes, and stirred at 250 rpm with a magnetic stirrer. The PU sponges were then removed from the ethanol, cleaned with distilled water, then oven-dried at 70°C for three hours. The PU sponge surfaces were modified using an aqueous suspension prepared by slowly transferring 0 g, 0.5 g, 1 g, 1.5 g, 2 g, or 2.5 g GNP into 400 mL distilled water stirred at 300 rpm using a magnetic stirring plate. After 10 minutes, the beaker that contained the resulting GNP aqueous suspension was placed in an ultrasonic bath and for ultrasonication at 30°C, 90 W, and 37 kHz for 90 minutes. Subsequently, 15 pieces of the cleaned PU sponges were submerged in the GNP aqueous suspension and the ultrasonication was continued for another 40 minutes as the interaction time. Subsequently, the GNP-coated PU sponges were removed from the aqueous suspension and oven-dried at 70°C for four hours before proceeding undergoing FTIR spectroscopic analysis, water and oil absorption capacity testing, and surface morphology examination.

2.3 The FTIR spectroscopy

The FTIR spectra of GNP, uncoated PU sponges, and GNP-coated PU sponges were acquired using an attenuated total reflectance (ATR)-FTIR spectrometer (Model Spectrum 100, Perkin Elmer). The spectra were recorded in the 4000–525 cm⁻¹ frequency range at 4 cm⁻¹ resolution and 16-scan accumulation. The FTIR spectra peak was assigned based on the reported works [14–17].

2.4 Measurement of water absorption capacity

The hydrophobicity of the uncoated and GNP-coated PU sponges was evaluated through the water absorption capacity test. A PU sponge with lower absorption capacity would demonstrate higher hydrophobicity. The water absorption capacity test was conducted following the method used by Zhang and co-workers [5], with slight modifications. First, the dry sponge mass (M_{W1}) was measured using an analytical balance. Subsequently, 80 mL distilled water was transferred to a 100 mL beaker, and the dry sponge was gently placed on the surface of the distilled water. After 5 minutes, the sponge was removed from the beaker at a 90° angle, and the excess water was allowed to drip for 10 seconds before the wet sponge mass (M_{W2}) was measured using analytical balance again. The water absorption capacity was then calculated according to Equation 1.

$$\text{Water absorption capacity (g/g)} = \frac{M_{W2} - M_{W1}}{M_{W1}} \quad (1)$$

2.5 Measurement of oil absorption capacity

The oil absorption capacity of the uncoated and GNP-coated sponges was measured through the oil absorption capacity test using the palm cooking oil and engine oil. The two oils were used to simulate the common oil water pollutions in the community. The palm cooking oil was used to simulate the water bodies polluted by the consumable oil discharged from households and the food processing industry. The engine oil was used to simulate the water bodies polluted by vehicle oil leaks from car workshops. The oil absorption capacity test was conducted following the method used by Zhang and co-workers [5], with slight modifications. Initially, the dry sponge mass (M_{O1}) was determined using an analytical balance. Subsequently, 40 mL distilled water was transferred to a 100 mL beaker and topped with 40 mL palm cooking oil. The liquids were equilibrated for 1 minute before the dry sponge was gently placed on the oil surface for oil absorption. After 5 minutes, the sponge was removed from the beaker at a 90° angle, and the excess oil was allowed to drip for 10 seconds before the wet sponge mass (M_{O2}) was measured. The oil absorption capacity of the PU sponges was calculated using Equation 2. The procedures were repeated by replacing the palm cooking oil with engine oil.

$$\text{Oil absorption capacity (g/g)} = \frac{M_{O2} - M_{O1}}{M_{O1}} \quad (2)$$

2.6 Examination of surface morphology

The surface morphology of the uncoated and GNP-coated PU sponges was examined using a Swift SW350T Compound Trinocular Microscope at $\times 40$ magnification. The microscopic images were captured, and the strut widths of the PU sponge cells were randomly measured at ten different regions using Motic Images Plus 3.0.

3. Results and discussion

3.1 The FTIR spectroscopic analysis

Figure 1 presents the FTIR spectra of the GNP and uncoated and GNP-coated PU sponges. The GNP spectrum demonstrated that alkyne C≡C bond stretching was recorded at 2325.37 cm⁻¹ and 2113.75 cm⁻¹, whereas alkyne ≡C-H bending was observed at 595.05 cm⁻¹. The absorption peak at 1990.86 cm⁻¹ reflected the presence of allene C=C=C bond stretching in the GNP. The confirmation of these hydrocarbon chromophores through the spectra confirmed that the GNP was mainly comprised of carbon atoms as the backbones in the graphene sheets.

The C-H and C-O-C stretching of PU polymer chains in the uncoated PU sponge was from the spectra at 2971.23 cm⁻¹ and 1222.61 cm⁻¹, respectively. Additionally, the absorption peaks at 1711.09 cm⁻¹ and 1537.59 cm⁻¹ were attributed to the carbonyl group (C=O) and N-H of carbamate (urethane) bond, respectively, was the resulting covalent bond due to the polymerisation between the hard and soft PU segments. The presence of intermolecular hydrogen bonds within the PU sponges via the interaction between the (i) hydroxyl groups (O-H) among the soft segment polyols, (ii) N-H among the carbamate bonds, and (iii) hydroxyl groups (O-H) of polyols and N-H of carbamate bonds, was observed through the absorption at the 3285.5 cm⁻¹ frequency. The

O-H bending and C-O stretching vibrations at 1092.04 cm^{-1} , 1295.21 cm^{-1} , and 1373.65 cm^{-1} indicated the existence of other hydroxyl groups (O-H) on the PU sponge surface.

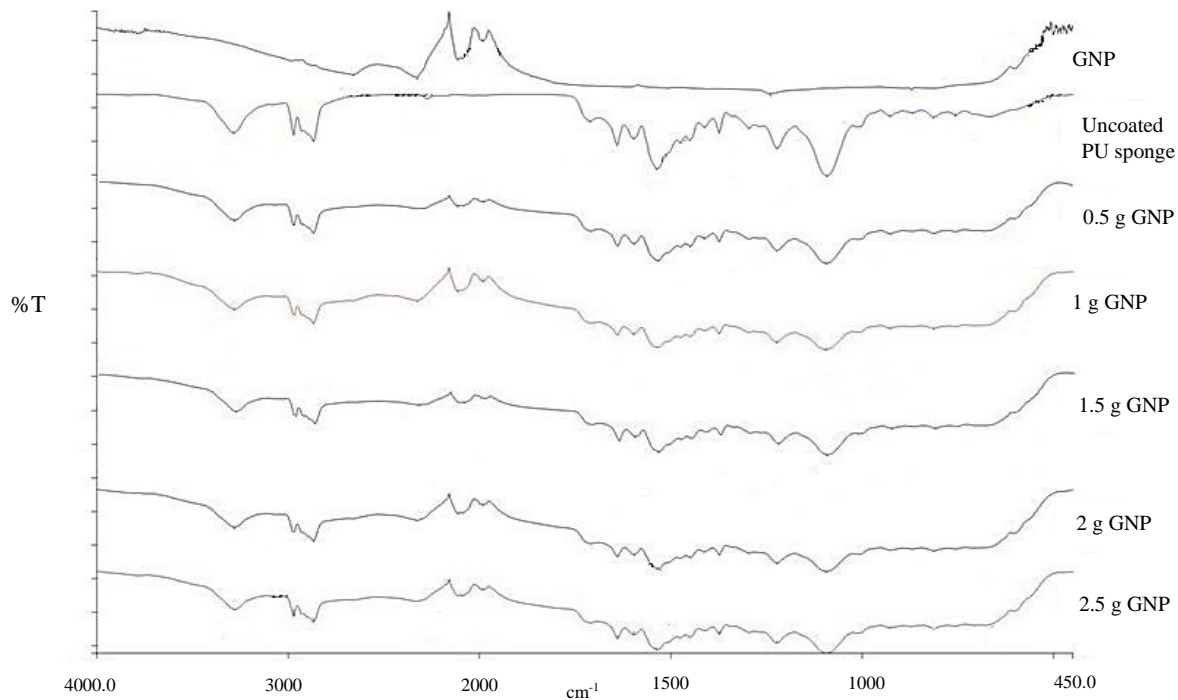


Figure 1 FTIR spectra of GNP and GNP-coated sponges.

The examination revealed that the GNP-coated PU sponge spectra demonstrated the characteristic peaks of both GNP and uncoated PU sponges. Nonetheless, the surface modification decreased the intensity of the characteristic peaks of the PU sponge. The coated PU sponge surface had a lower intensity of the C-H (2971.23 cm^{-1}) and C-O-C stretching (1222.61 cm^{-1}) of the PU polymer chains, the C=O (1711.09 cm^{-1}) and N-H (1537.59 cm^{-1}) of carbamate (urethane) bond, intermolecular hydrogen bonds within the PU sponges (3285.5 cm^{-1}), and the O-H bending and C-O stretching vibration (1092.04 cm^{-1} , 1295.21 cm^{-1} , and 1373.65 cm^{-1}) of the hydroxyl groups (O-H) than the uncoated PU sponge. This observation was clarified by the GNP coating on the PU sponge surface, which covered and reduced the light absorption by the PU sponge chromophores. This observation was consolidated through the presence of the characteristic peaks of GNP, which were absent from the uncoated PU sponge spectrum. For the GNP-coated PU sponges, the GNP absorption peaks were observed through the alkyne C≡C bond stretching at 2325.37 cm^{-1} and 2113.75 cm^{-1} , alkyne ≡C-H bending at 595.05 cm^{-1} , and the allene C=C=C bond stretching at 1990.86 cm^{-1} . Thus, the spectra confirmed that the GNP was coated onto the PU sponge surface through the dip-coating.

3.2 Water absorption capacity

Table 1 shows the water absorption capacity of the modified PU sponges. The uncoated PU sponge had the highest water absorption capacity, which was equivalent to 0.646 g/g . This observation was expected as the uncoated PU sponge is hydrophilic due to the presence of abundant free hydroxyl groups on the sponge surface. Nevertheless, the water absorption capacity began to decline to 0.615 g/g when the PU sponge surfaces were modified using the aqueous suspension containing 0.5 g GNP , which was attributed to the GNP deposition on the PU sponge surfaces.

Table 1 Water absorption capacity of the GNP-coated PU sponges.

Amount of GNP (g)	Water absorption capacity (g/g)
0	0.646 ± 0.051
0.5	0.615 ± 0.250
1.0	0.229 ± 0.000
1.5	0.183 ± 0.024
2.0	0.179 ± 0.061
2.5	0.073 ± 0.104

The GNP repelled water due to its inherent hydrophobicity. With 1 g GNP, the water absorption capacity of the sponge decreased significantly to 0.229 g/g, which was further reduced to 0.183 g/g, 0.179 g/g, and 0.073 g/g when 1.5 g, 2 g, and 2.5 g GNP were used. This result demonstrated that increasing the GNP amounts increased the hydrophobicity of the PU sponges. The hydrophobicity of the modified PU sponges was mainly attributed to the coating of hydrophobic GNP, which naturally repels water. As the modification process involved higher amounts of GNP, more GNP was coated onto the PU sponge surfaces, which increased the hydrophobicity of the modified sponges. Increasing the amount of GNP coated on the sponge also covered more hydroxyl groups on the PU sponge surfaces, which rendered them less accessible by the water molecules and thus increased the hydrophobicity.

3.3 Palm cooking oil and engine oil absorption capacity

Figure 2 depicts the amount of palm cooking oil and engine oil absorbed by the GNP-coated PU sponges. The uncoated PU sponge was simply cleaned with ethanol, washed, and dried without any GNP coating (0 g). Expectedly, the uncoated PU sponge had the lowest absorption capacity of palm cooking oil (5.63 g/g) and engine oil (3.16 g/g). Contrastingly, the sponge coated with 1 g GNP had the highest absorption capacity for palm cooking oil and engine oil, which were 44.02 g/g and 43.55 g/g, respectively, which was followed by that of the PU sponge coated with 0.5 g GNP (42.29 g/g for palm cooking oil and 42.57 g/g for engine oil). The substantial increase in the oil absorption of the PU sponge was attributed to the amount of GNP coating the PU sponge. The GNP has non-polar sp^2 hybridized carbon atoms and a symmetric hexagonal lattice structure, which results in an affinity for non-polar oil molecules.

The affinity of PU sponges for oil molecules increased together with the amount of GNP used during the dip-coating. Therefore, the oil absorption of the PU sponges increased when the amount of GNP increased from 0.5 g to 1 g. The observation aligned with the water absorption capacity reported earlier. After the peak, the oil absorption capacity steadily decreased when the amount of GNP increased to 2.5 g. The absorption capacity of the PU sponge modified with 1.5 g GNP was 40.71 g/g for palm cooking oil and 38.96 g/g for engine oil. The oil absorption capacity further decreased to 40.51 g/g for palm cooking oil and 38.83 g/g for engine oil, 37.25 g/g for palm cooking oil and 38.79 g/g for engine oil in the sponges coated with 2 g and 2.5 g GNP, respectively. The decreasing trend in oil absorption capacity was clarified by the agglomeration of GNP particles on the PU sponge surface, which reduced the effective surface area of GNP interaction with oil molecules. Furthermore, the GNP agglomerates also reduced and blocked the sponge cells and hindered the diffusion of oil molecules into the inner surface PU sponge cells and reduced the oil absorption accordingly. Thus, using more GNP during the surface modification increased the size of GNP agglomerates formed. Consequently, the oil absorption capacity declined when the amount of GNP was increased from 1 g to 2.5 g.

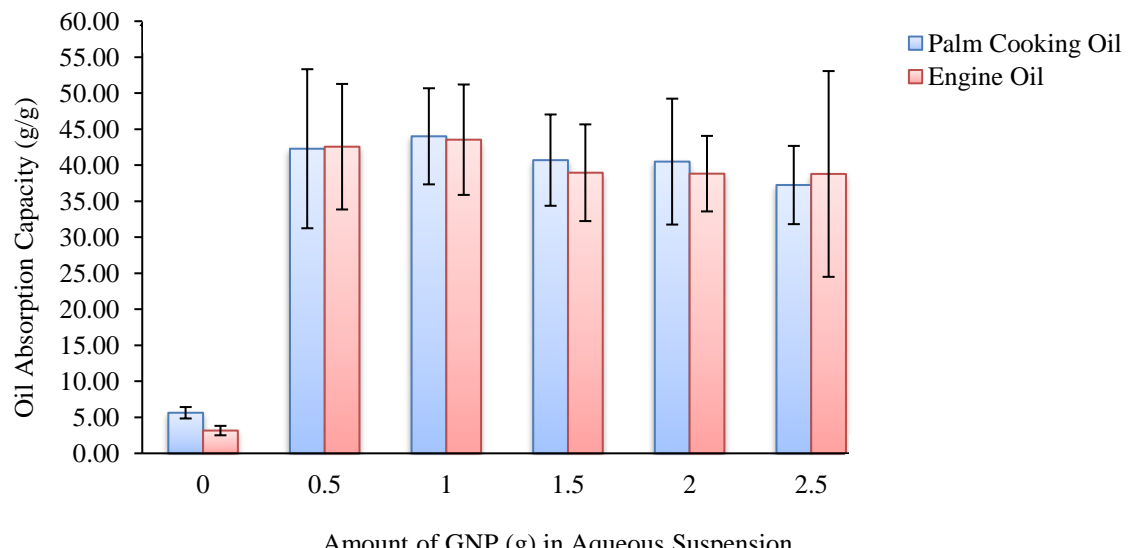


Figure 2 Absorption capacity of palm cooking oil and engine oil of the GNP-coated PU sponges.

The highest oil absorption capacity was achieved by coating the PU sponge with 1 g GNP. The oil absorption capacity of the GNP-coated PU sponge was 44.02 g/g for palm cooking oil and 43.55 g/g for engine oil, which was almost equivalent to 44 times its dry mass. This oil absorption capacity was higher than that of the graphene-coated PU sponge prepared by Zhang and co-workers [5], which was 29 times for olive oil and 31 times for lubricant. Additionally, the oil absorption capacity of the GNP-coated PU sponges was also higher than that

of the graphene oxide-coated PU sponge reported by Xia and co-workers [10], which was approximately 38 times for soybean oil and 29 times for gasoline.

3.4 Surface morphology

Figure 3(A) presents the open-cell structure of the uncoated PU sponge, which features a clean and smooth 3D open-cell porous structure. Nonetheless, when 0.5 g GNP was used, the GNP was coated on the corner, strut, and node of the PU sponge cells. The GNP coating on the sponge surface increased the roughness of the 3D network. The microscopic image confirmed that the GNP coating on the PU sponge surface conferred hydrophobicity to the sponge and significantly increased its oil absorption capacity. Increasing the amount of GNP to 1 g significantly increased the amount of GNP coated on the PU sponge. This observation confirmed the highest oil absorption capacity of the PU sponge reported in the previous section. Nonetheless, the microscopic images also demonstrate that the GNP was unevenly dispersed, began to agglomerate, and clustered together when higher amounts of GNP were used. Some of the cells were even extensively covered by GNP agglomerated fragments and were reduced in size. This observation became apparent when the amount of GNP was increased from 1.5 g to 2.5 g. Consequently, the GNP agglomeration and reduced cell size exerted adverse effects on the diffusion of oil molecules into the 3D networks of the PU sponge and reduced the oil absorption capacity reported in the earlier section. This observation was further consolidated by FTIR spectroscopic analysis presented in Section 3.1, which confirmed that the amount of GNP deposited on the sponge surfaces increased proportionally with the amount of GNP used during the dip-coating.

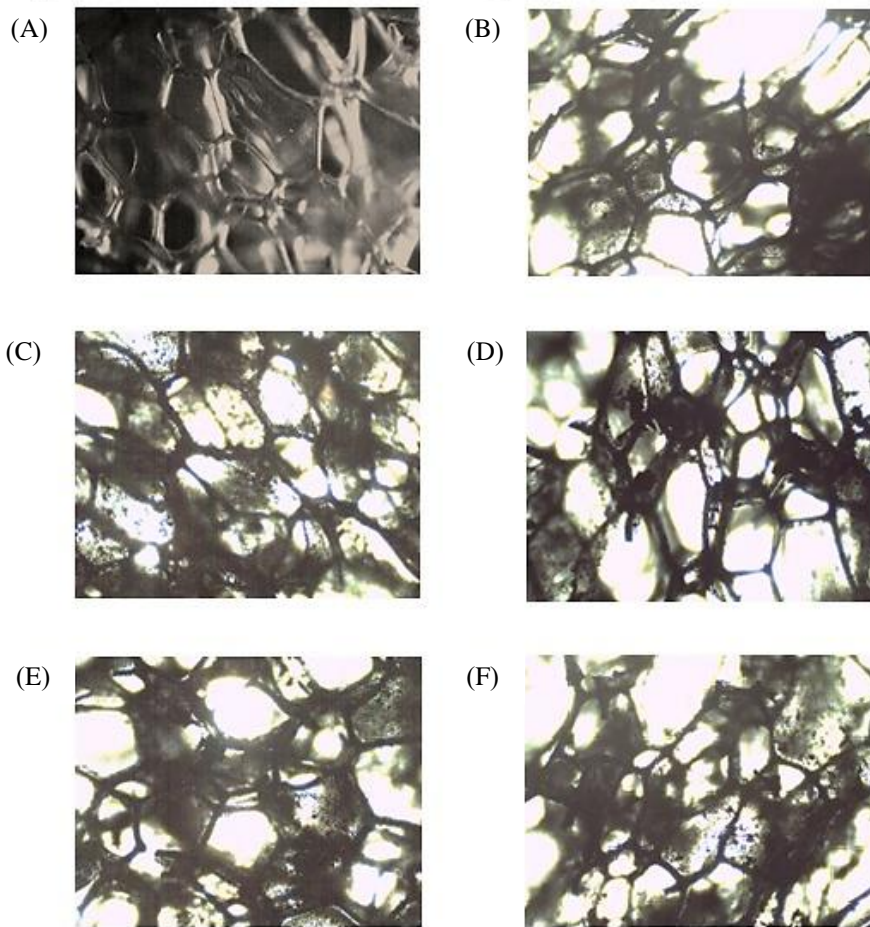


Figure 3 Surface morphology of GNP-coated PU sponges prepared using (A) 0 g, (B) 0.5 g, (C) 1 g, (D) 1.5 g, (E) 2 g, and (F) 2.5 g GNP.

To further support the observations of surface morphology, the strut widths of both uncoated and GNP-coated PU sponge cells were measured, as shown in Table 2. The uncoated PU sponge had the smallest strut width, approximately 60.82 μm . After modification with aqueous suspensions containing 0.5 g and 1 g of GNP, the strut widths increased to 63.46 μm and 68.44 μm , respectively. This increase was attributed to the deposition of GNP

on the PU sponge surfaces during the dip-coating. The thickening of the struts confirmed the successful GNP coating, further supporting the microscopic observations in Figures 3(B) and 3(C).

The uneven dispersion and agglomeration of GNP observed in Figures 3(D), 3(E), and 3(F) were also consistent with the strut width measurements. The strut widths of the PU sponge cells further increased to 72.79 μm , 76.82 μm , and 80.12 μm when the amount of GNP was increased to 1.5 g, 2 g, and 2.5 g, respectively. Moreover, the PU sponges modified with 2 g and 2.5 g GNP aqueous suspension exhibited a wider range in the standard deviation of their strut widths. This variation suggested significant fluctuations and inconsistencies in strut thickness, likely due to the uneven dispersion and deposition of GNP agglomerates on the sponge surfaces. These findings further supported the surface morphology analysis.

Table 2 Strut widths of the GNP-coated PU sponges.

Amount of GNP (g)	Strut widths of PU sponge cells (μm)
0	60.82 \pm 5.04
0.5	63.46 \pm 13.41
1.0	68.44 \pm 10.37
1.5	72.79 \pm 9.36
2.0	76.82 \pm 28.32
2.5	80.12 \pm 21.93

4. Conclusions

This study successfully modified PU sponges using GNP. The FTIR spectrum confirmed the successful coating of the hydrophobic, oleophilic GNP onto the PU sponge and enhanced the hydrophobicity and oleophilicity to the PU sponge. The palm cooking oil and engine oil absorption of the PU sponge was significantly enhanced by 681.88% and 1278.16%, respectively, and maximum oil absorption capacity was achieved when 1 g GNP was used. The enhancement in oil absorption was accompanied by a remarkable reduction in water absorption, which indicated the improved hydrophobicity of the GNP-coated PU sponge. Ultimately, this study confirmed that 1 g GNP should be used for PU sponge surface modification due to its optimum oil absorption and its even dispersion, as evidenced by the surface morphology examination.

5. Acknowledgements

This research was supported by Taylor's University through the Taylor's Internal Research Grant Scheme - Impact Lab Grant (TIRGS-ILG) (Project Code: TIRGS-ILG/1/2023/SOE/002).

6. Author Contributions

Mitchell, S.: Formal analysis, Investigation, Methodology, Project administration, Writing – original draft; Low, JH.: Conceptualization, Funding acquisition, Methodology, Project administration, Supervision, Writing – review & editing; Yoon, LW.: Conceptualization, Supervision

7. Conflicts of interest

The authors declare no conflicts of interest relevant to the content of this article.

8. References

- [1] Aguilera F, Méndez J, Pásaro E, Laffon B. Review on the effects of exposure to spilled oils on human health. *J Appl Toxicol*. 2010;30(4):291–301.
- [2] Kabiri S, Tran DNH, Altalhi T, Losic D. Outstanding adsorption performance of graphene–carbon nanotube aerogels for continuous oil removal. *Carbon*. 2014;80:523–533.

- [3] Diraki A, Mackey H, McKay G, Abdala AA. Removal of oil from oil–water emulsions using thermally reduced graphene and graphene nanoplatelets. *Chem Eng Res Des*. 2018;137:47–59.
- [4] Doshi B, Sillanpää M, Kalliola S. A review of bio-based materials for oil spill treatment. *Water Res*. 2018;135:262–277.
- [5] Zhang X, Liu D, Ma Y, Nie J, Sui G. Super-hydrophobic graphene coated polyurethane (GN@PU) sponge with great oil–water separation performance. *Appl Surf Sci*. 2017;422:116–124.
- [6] Kumar M, Sachdeva A, Garg RK, Singh S. Using RSM to optimize crystallite size of rice husk derived graphene prepared by microwave process. *Asia Pac J Sci Technol*. 2022;27(06):20-27.
- [7] Vaka M, Walvekar R, Khalid M, Jagadish P, Low JH. Corrosion, rheology, and thermal ageing behaviour of the eutectic salt-based graphene hybrid nanofluid for high-temperature TES applications. *J Mol Liq*. 2021;334:116156.
- [8] Karm Z. A comparative study of the structure and morphology of graphene oxide films on glass and aluminum supports by using dip coating. *Asia Pac J Sci Technol*. 2024;29(05):20-29.
- [9] Liu H, Liu Z, Yang M, He Q. Surperhydrophobic polyurethane foam modified by graphene oxide. *J Appl Polym Sci*. 2013;130(5):3530–3536.
- [10] Xia C, Li Y, Fei T, Gong W. Facile one-pot synthesis of superhydrophobic reduced graphene oxide-coated polyurethane sponge at the presence of ethanol for oil–water separation. *Chem Eng J*. 2018;345:648–658.
- [11] ACS Material LLC. 5th ed. A Detailed Overview of Graphene Nanoplatelets. 2020
- [12] Yee K, Ghayesh MH. A review on the mechanics of graphene nanoplatelets reinforced structures. *Int J Eng Sci*. 2023;186:103831.
- [13] Cheong KL, Pang MM, Low JH, Tshai KY, Koay SC, Wong WY. Graphene nanoplatelets/polylactic acid conductive polymer composites: tensile, thermal and electrical properties. *Chem Eng Technol*. 2024;47(11):e202300592.
- [14] Ng QY, Low JH, Pang MM, Idumah CI. Properties enhancement of waterborne polyurethane bio-composite films with 3-aminopropyltriethoxy silane functionalized lignin. *J Polym Environ*. 2023;31(2):688–697.
- [15] LG Wade JR. Organic chemistry. 7th ed. Upper Saddle River: Pearson Education, Inc.; 2010.
- [16] Aris NF, Ghazali SK, Mohamad Z, Jamaluddin J, Adrus N, Abdul Aziz A. The effects of alkaline treatment on the oil residue, thermal properties and surface morphology of oil palm mesocarp fiber. *Environ Qual Manag*. 2022;32(1):405–411.
- [17] Rusman R, Majid RA, Wan Abd Rahman WA, Low JH. Carboxymethyl cassava starch/polyurethane dispersion blend as surface sizing agent. *Chem Eng Trans*. 2017;56:1171–1176.